Virtual screening for potential inhibitors of Lassa fever nucleoprotein

*Amaku James Friday, Kalu Kalu Igwe and Buhari Magaji

Abstract *The devastating impact of viral haemorrhagic fevers has deeply been felt in South America and Africa. This fever is caused by the arenaviruses Lassa and has posed a matchless fight. Meanwhile, no effective drug or vaccine has been reported. Here we used virtual screening and molecular docking approach to identify a series of novel inhibitors (ZINC64450313 (-10.7 kcal/mol), ZINC00658482 (-10.5 kcal/mol), ZINC40789449 (-10.5 kcal/mol), ZINC14551223 (10.0 kcal/mol) and ZINC73892903 (10.0 kcal/mol)) that can exhibit significant binding affinity to Lassa fever nucleoprotein (PDB ID: 3mx5) than ribavirin (-6.7 kcal/mol). Swiss ADME web tools were used to assess the pharmacokinetics   and   drug-likeness characteristics   of   the   lead   molecule (ZINC64450313).   This assay showed that ZINC64450313 obeyed Lipinski, Egan, Verber and Muegge rules. However, pharmacokinetics predictions indicated that CYP1A2, CYP2C9, CYP2D6 and CYP2C19 isoenzyme were not inhibited by ZINC64450313. Toxicity assay of ZINC64450313 was acquired with an average similarity index of 33.25% and prediction accuracy of 23% on the ProTox-II webserver. The lead molecule has an LD50 value of 10 mg/kg and belongs to toxicity class 2. The frontier molecular orbital's analysis revealed that ZINC64450313 is more reactive than ribavirin due to the possesion of better quantum chemical indices such as its the global hardness. Hence, an in vitro and in vivo assay of these molecules may proffer a pathway to finding effective inhibitors with the potential to truncate functional proteins responsible for the viral life cycle of arenaviruses Lassa.*

*Amaku James Friday
Department of Chemistry,
Michael Okpara University of Agriculture,
Umudike, Abia State, Nigeria
Email: amakufj2006@gmail.com
Orcid id: 0000-0003-4894-0512

Kalu Kalu Igwe
Departmemt of Veterinary Physiology,
Pharmacology and Biochemistry
Michael Okpara University of Agriculture,
Umudike, Abia State, Nigeria
Email: kkigwe191@gmail.com
Orcid id: 0000-0002-8118-5689

Buhari Magaji
Department of Chemistry, Faculty of Science,
Gombe State University, Gombe State
Email: magaji.buharii@gmail.com
Orcid id: 0000-0002-2413-3890

1.0   Introduction

Lassa virus (LASV) is the causative agent of Lassa hemorrhagic fever, a member of the *Arenaviridae* family of viruses (Houlihan and Behrens, 2017; Zhang *et al*., 2019).   It is responsible for 200,000 human infections and around 5000 deaths in West Africa per annum. Available literature reveal that more than 20 cases of Lassa fever have been reported in Japan, Europe, and North America (Shimojima *et al.,* 2012).   At present, there is no FDA-approved LASV-specific drugs or vaccines.   However, ribavirin is the sole antiviral drug used for LASV management, it is commonly used for treatment at the early phase (McCormick *et al*., 1986). Also, the combined therapy of ribavirin with favipiravir demonstrated   significant   synergistic physiological implication in the in LASV-infected mice (Carrillo-Bustamante *et al*., 2017).

The primary host for Lassa virus is *Mastomys natalensis*, a species of rodent that is commonly found in domestic residence (Monath *et al*., 1974). However, the transmission of this disease to human is *via* Virus-contaminated urine from *Mastomys natalensis* while human-to-human transmission is through contact with the body fluids of infected patients (Keenlyside *et al*., 1983). LASV is an enveloped RNA virus and is known to express four viral proteins namely, viral polymerase (L), matrix protein (Z), nucleoprotein (NP), and the glycoprotein complex (GPC) (Hastie *et al.*, 2017). The viral binding to and entry into cells is a function of the glycoprotein

precursor (Zhang *et al*., 2019). Prior to the binding, the GPC is first synthesized as a mono-polypeptide that dissociate into three segments, namely, the stable signal peptide (SSP), the receptor-binding subunit (GP1), and the membrane fusion subunit (GP2). These subunits bound together to form trimers that are packed onto the virion surface (Bederka *et al*., 2014).

The devastating impact of LASV is observed on its early attack on dendritic cells, macrophages and endothelial cells, thus, interfering with the activities of inflammatory mediators (Baize *et al*., 2004; Lukashevich *et al*., 1999; Mahanty *et al*., 2003). Studies revealed that the LASV can causes damages to the liver, adrenal gland, kidney, lung, spleen, and heart (McCormick *et al*., 1986; Sbrana *et al*., 2006; Walker *et al*., 1982). Due to increase in number of reported cases of Lassa infections in Africa and lack of efficacious therapeutics, the need to develop antiviral drugs for the treatment of this virus is necessary and is receiving serious research attention. However, drug repurposing has become a well-known approach in the field of drug discovery with the aim to fast-track the development process (Ashburn & Thor, 2004). This approach has been successfully used to identify effective inhibitors for Ebola, Zika, and severe acute respiratory syndrome (SARS) virus inhibitors, with several promising hit/lead-antivirals, reported (Cheng, Murray, & Rubin, 2016; Dyall *et al*., 2014; Johansen *et al*., 2015; Kouznetsova *et al*., 2014; Madrid *et al*., 2013). Therefore, the present study seeks to employed pharmacophore virtual screening of ZINC database, a computer-aided drug design (CADD) technique to search for LASV inhibitors in which clinically approved drug (ribavirin) is used as pharmacophore reference.

2.0   Materials and Methods
2.1   *Structure-based virtual screening*
The simplified molecular-input line-entry (SMILE) of ribavirin was obtained from the drug bank online platform. The UCSF Chimera interface was used to convert the SMILE format of ribavirin into its 3D model before submission to ZINCPharmer with distinct pharmacophoric features (Koes & Camacho, 2012; Morris *et al*., 1998; Pettersen *et al.*, 2004). The model molecule (ribavirin) was added to ZINCPharmer with distinct criteria (molecular weight of <500 Da, hydrogen bond donors <5, hydrogen bond acceptors <10 and rotatable bonds <6), to screen the ZINC database for the potential 3mx5 inhibitors (Koes & Camacho, 2012; Morris *et al*.,

1998; Pettersen *et al*., 2004). Based on the generated pharmacophore features of ribavirin, the ZINC database was screened to obtain drug-like compounds with similar pharmacophoric features as exhibited by ribavirin. The 2D conformation of the predicted small molecules (inhibitors) retrieved from the ZINC database was optimized using the MMF94 force field on Avogadro interface (Hanwell *et al*., 2012). Prior to the molecular docking step, the optimized 3D structures of the acquired molecules were processed by making use of the dock-prep tools on the UCSF Chimera interface.

2.2   *Molecular docking*
The complexed crystalized structure of Lassa fever nucleoprotein was retrieved from the Protein Data Bank with ID 3mx5. The structure of Lassa fever nucleoprotein was noticed to have distinct chains A, B and C bounded together and complexed with a ligand (ID: UTP). The preparation of the biological target (receptor/3mx5) acquired from the protein data bank was executed on the UCSF Chimera interface, in which the small molecule complexed to the protein was removed and the region used as pocket/site for docking (Pettersen *et al.*, 2004). To further evaluate the drugable capacity of all the retrieved compounds, molecular docking assay was performed on all the hits obtained from the ZINC database to predict their binding conformation and affinity within the active site region of 3mx5. Ligand-receptor docking was achieved by making use of the AutoDock Vina software (Morris *et al*., 1998). The grid box that defines the binding active site region of 3mx5 protein was estimated from the AutoDock Vina functionality on UCSF Chimera (Pettersen *et al.*, 2004). The grid box size and centre coordinates for the protein were x(58.4425, 10.2261), y (64.3139, 9.48734) and z (20.2236, 10.000) respectively. The compound with higher binding affinity than the reference inhibitor (Ribavirin) was considered for further analysis.

2.3   *Validation and ADMET analysis of hits compounds*
The ADME properties of the lead inhibitor (ZINC64450313) was assessed by making use of online SwissADME tool (Monteiro *et al*., 2019). This tool was also used to formulate the drug-like characteristic of ZINC64450313, from which the potential and effectiveness of this compound were established. The toxicity risks of ZINC64450313 was evaluated using ProTox-II webserver.

2.4   *Quantum chemical calculations*

The global reactivity descriptors of the lead molecule were calculated *via* quantum chemical calculations. This analysis was performed on Gaussian 09 equipped with Gaussview 5.0 software package (Gaussian09, 2009). In the present investigation, the Becke–Lee Yang–Parr functional (B3LYP) method with 6-311++G (d, p) basis sets (Becke, 2005) were employed. The structure of the small molecules was optimized before energy estimation. Electronic transitions in the UV-Vis spectral region were determined by time-dependent (TD) DFT method with B3LYP level and 6-311++G (d, p) basis set. The frontier molecular orbitals energies were also assessed and used to estimate reactivity descriptors such as electronegativity (χ), hardness (η), softness (S) and electrophilicity index (ω). The energy gap (ΔE) was calculated as the difference between LUMO and HOMO energies (Koopmans, 1934; Pandey, Muthu and Gowda, 2017; Yang and Parr, 1985). The ionization potential (IP $\approx$ - E_{HOMO}) and electron affinity (EA $\approx$ - E_{LUMO}) were applied to the following equations in the estimation of the global reactivity descriptors (Ayers and Levy, 2000; Chattaraj, *et al.*, 2009; Chermette, 1999; Gazquez et al., 2007; Geerlings *et al.*, 2003).

Electronegativity $(\chi) = \frac{IP + EA}{2}$ (1)

Hardness $(\eta) = \frac{IP - EA}{2}$ (2)

Softness $(S) = \frac{1}{\eta}$ (3)

Chemical potential, $(\mu) = -\frac{IP - EA}{2}$ (4)

Electrophilicity index $(\omega) = \frac{\mu^2}{2\eta}$ (5)

3.0 Results and Discussion
3.1 Pharmacophore-based virtual screening and database preparation
The ZINC database was screened for hit compounds with similar pharmacophoric features of the reference molecule (Ribavirin). The key features of the reference molecule were selected by making use of ZINC pharmacophore. The 3D image of ribavirin showing the selected pharmacophoric signals is displayed in Fig. 1. As shown in Table 1, the pharmacophore key features with one hydrophobic, one aromatic and one H-accepter were chosen to design a pharmacophore model that was used to screen the ZINC database containing ~250 million compounds in 3D format. The X, Y and Z are the coordinates of the pharmacophoric signals of ribavirin as assigned by the ZINCpharmer search engine, these coordinates showed the dimension where these pharmacophoric signals are localized on the ribavirin molecule (see Table 1). From the result

obtained, 45 out of 100 hit compounds were retrieved and energy minimization was performed on all the compounds prior to the docking step.
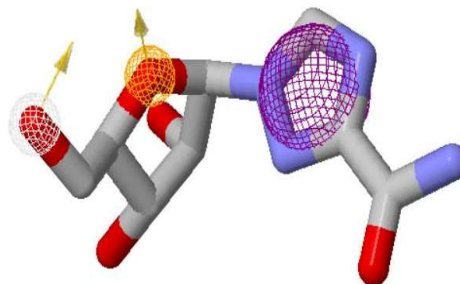
Fig. 1: The 3D image of Ribavirin showing the pharmacophoric signals on the ZINCPharmer online Platform.

Table 1: The dimensions of the pharmacophoric features of Ribavirin on ZINCpharmer platform.

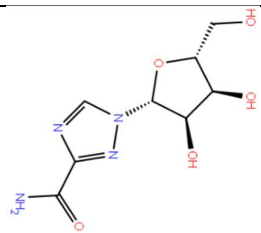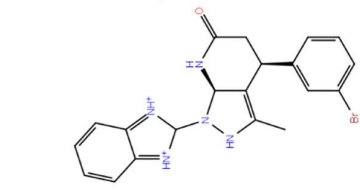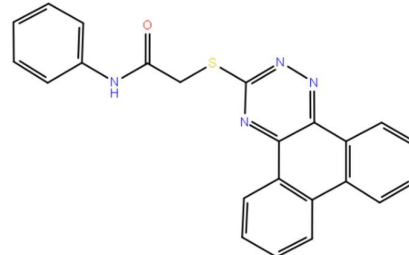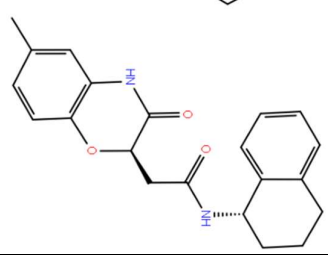| Pharmacophore Class	X	Y	Z	Radius
Hydrogen acceptor	7.40	10.07	6.86	050
Aromatic	7.80	7.06	8.20	1.10
Hydrophobic	8.92	11.29	4.65	0.50

3.2 Molecular docking
To further assess the prospects of the forty-five identified hit compounds, the binding modes and affinities of each compound were evaluated *via* molecular docking relative to the reference compound (Ribavirin). The binding affinities of the forty-five compounds were predicted by making use of the scoring functions associated with molecular docking process. Meanwhile, the lowest five docking scores, which indicates compounds with the best affinity for 3mx5 protein are presented in Table 2. Several reports suggest that the more negative the binding affinity of an inhibitor to its target, then the stronger the binding (Abdullahi *et al.,* 2018; Patil *et al.*, 2010). It was noticed from the molecular docking results that ZINC64450313,ZINC00658482,ZINC40789449, ZINC14551223 and ZINC73892903 exhibited favourable binding affinity of -10.7, -10.5, -10.5, -10.0 and -10.0 kcal/mol respectively. The binding energy of ribavirin is -6.7 kcal/mol, which is less than those of the newly design molecules. Amongst these five compounds, ZINC64450313 showed the highest binding affinity against 3mx5 protein. The relative favourable binding affinity observed for these compounds indicates possible inhibitory activity on target organism. The

comparative binding interaction profiles of potential inhibitors and ribavirin were a crucial part of the study because the interaction of these compounds with binding site residues influence the overall binding affinity of the compound within the binding site. It was observed that ZINC64450313 exhibited a higher number of interactions with binding site residues relative to ribavirin. A similar trend was observed for the ZINC00658482, ZINC40789449, ZINC14551223 and ZINC73892903. Pocket interaction analysis revealed that ZINC64450313 interacted with nineteen amino acid residues (LUE 172, ASN 305, LYS 253, SER 238, ASN 240, ILE 241, TRP 164, LEU 120, GLU 117, ASN 174, ARG 323, PHE 176, GLY 177, THR 174,

LYS 309 and ARG 300) within the pocket of 3mx5. The high affinity of ZINC64450313-3mx5 could be attributed to the hydrogen bonds formed between the secondary amine of the pentacyclic fragment of ZINC64450313 with ILE 241 amino acid, hydrophobic interaction and possible interaction of ZINC64450313 with some heteroatoms of the polar amino acid residues within the pocket of 3mx5. On the contrary, hydrogen bonds formation was observed between the free hydroxyl moiety of ribavirin and ASN 174 and SER 238. Hence, the nature of ZINC64450313 interaction within the pocket of 3mx5 may have favoured its affinity for the receptor (see Figs. 2 and 3).

Table 2: The 2D representation, ZINC code and Glide score (G-Score) value calculated with respect to the related query, of the shared best 5 hits.
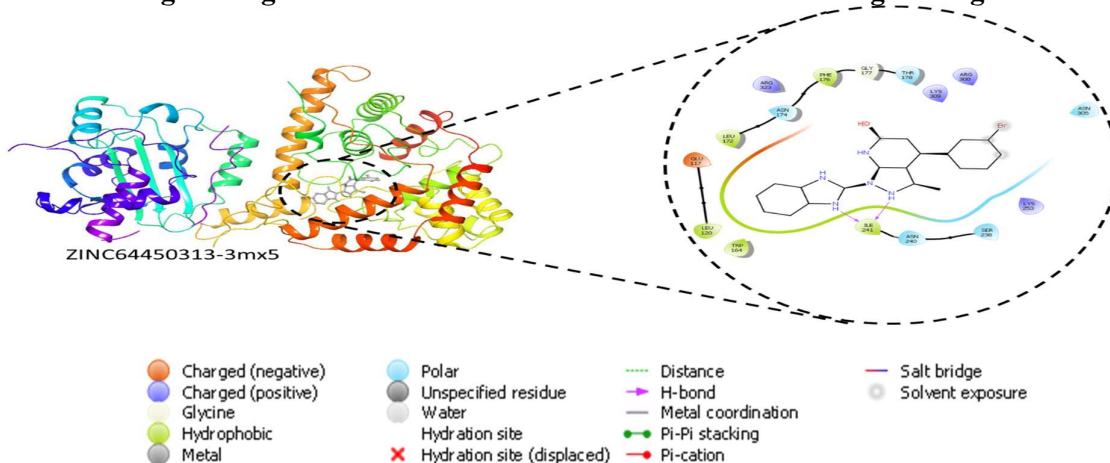
| CODE	SCORE *ΔG (Kcal/mol)	STRUCTURE
Ribavirin	-6.7	
ZINC64450313	-10.7	
ZINC00658482	-10.5	
ZINC40789449	-10.5	

| ZINC14551223 | -10 | |
| ZINC73892903 | -10 | |
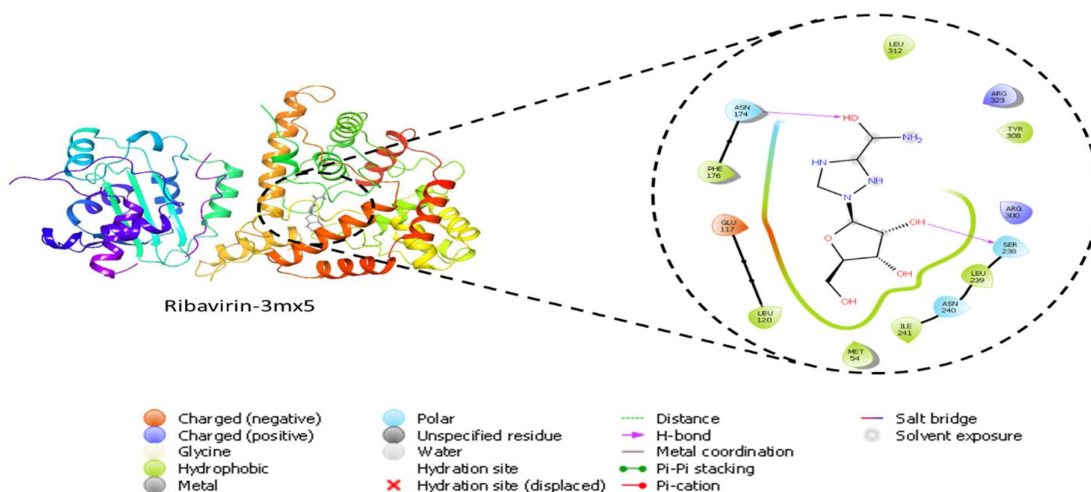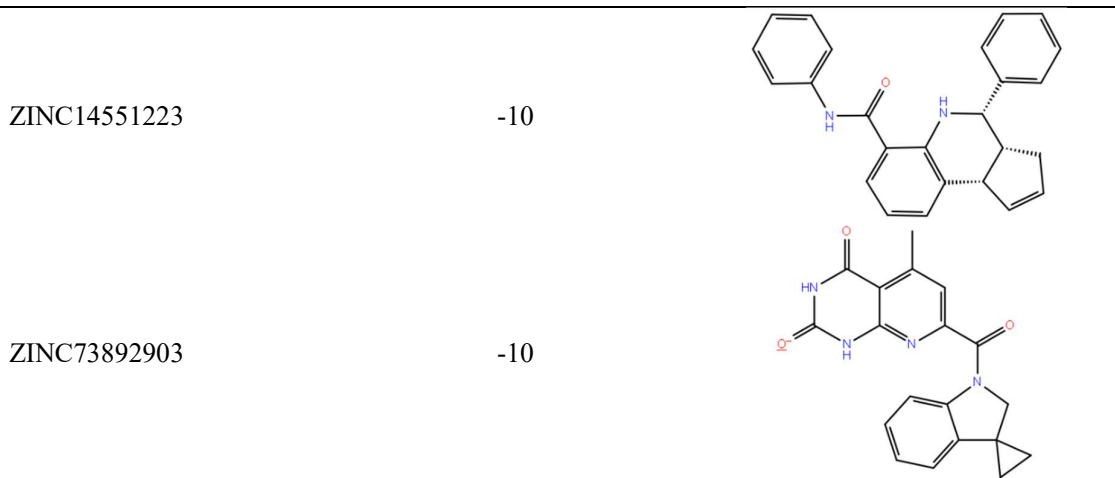
Fig.2.The 3D X-ray crystal structure of 5r7y complex with ribavirin showing also the binding site region and the residues that constitute this binding site region.
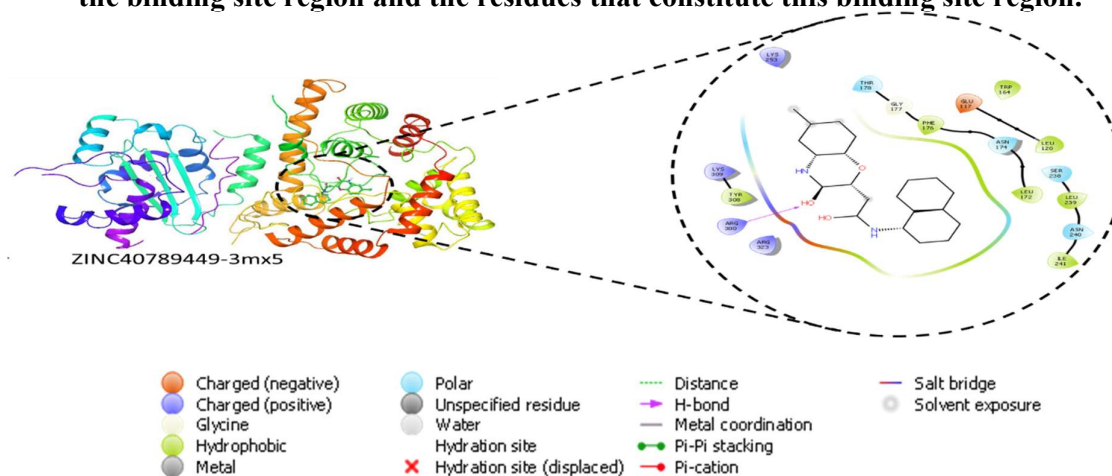

Fig.3.The 3D X-ray crystal structure of 5r7y complex with ZINC64450313 showing also the binding site region and the residues that constitute this binding site region.
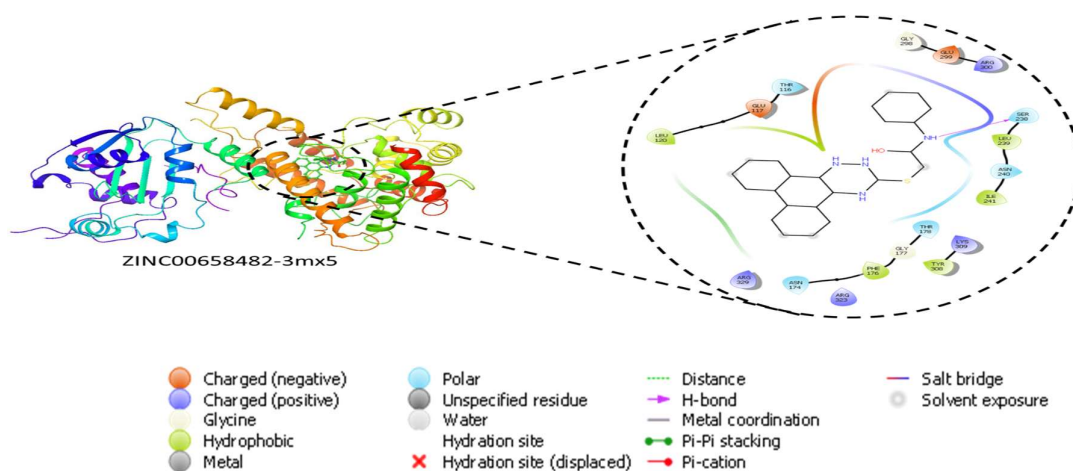
Fig.4.The 3D X-ray crystal structure of 5r7y complex with ZINC00658482 showing also the binding site region and the residues that constitute this binding site region.

Fig.5.The 3D X-ray crystal structure of 5r7y complex with ZINC40789449 showing also the binding site region and the residues that constitute this binding site region.

Fig.6.The 3D X-ray crystal structure of 5r7y complex with ZINC14551223 showing also the binding site region and the residues that constitute this binding site region.

Fig.7. The 3D X-ray crystal structure of 5r7y complex with ZINC73892903 showing also the binding site region and the residues that constitute this binding site region.
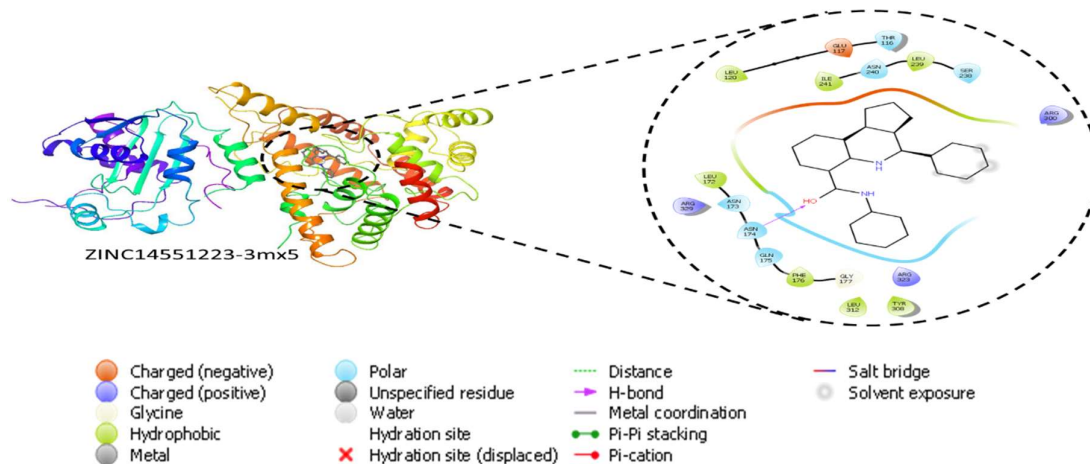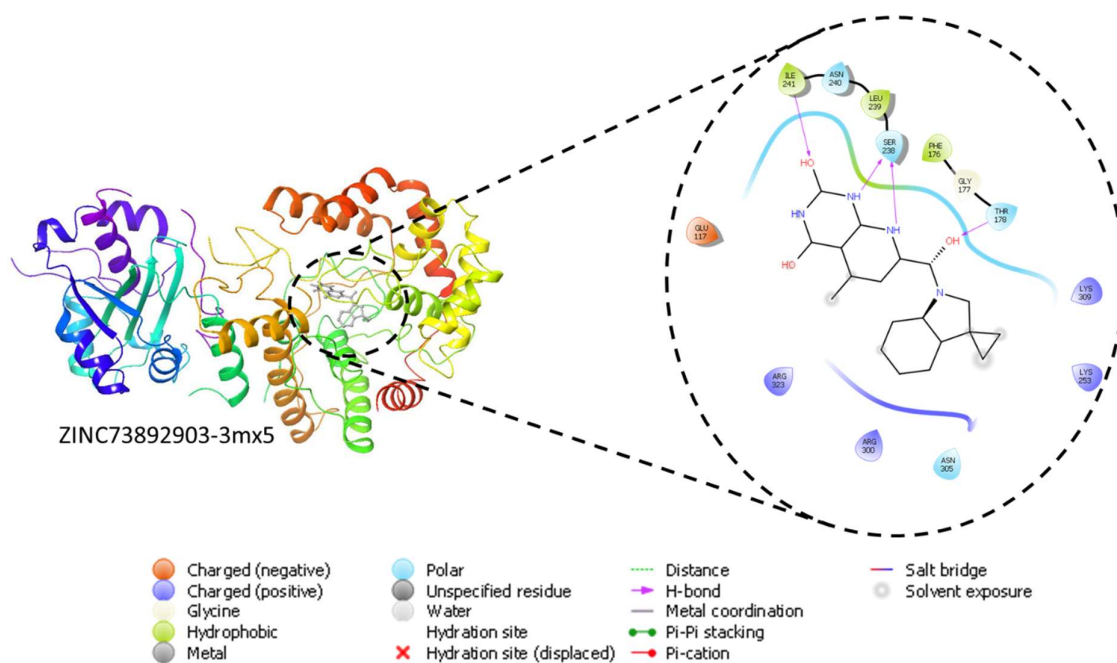
.

3.3 Pharmacokinetic assessment of potential Lassa fever nucleoprotien inhibitors

The potentials of ZINC64450313 as drug candidate was evaluated by making use of the online platform SwissADME to predict the pharmacokinetic properties, absorption, distribution, metabolism and excretion (ADME).

This was necessary to evaluate the prospects ZINC64450313 for human use. The oral bioavailability of ZINC64450313 is displayed in the coloured zone as shown in Fig. 8. The coloured zone shows viable 75 % physicochemical space of ZINC64450313 which was considered as lipophilicity, saturation, size, polarity and solubility.
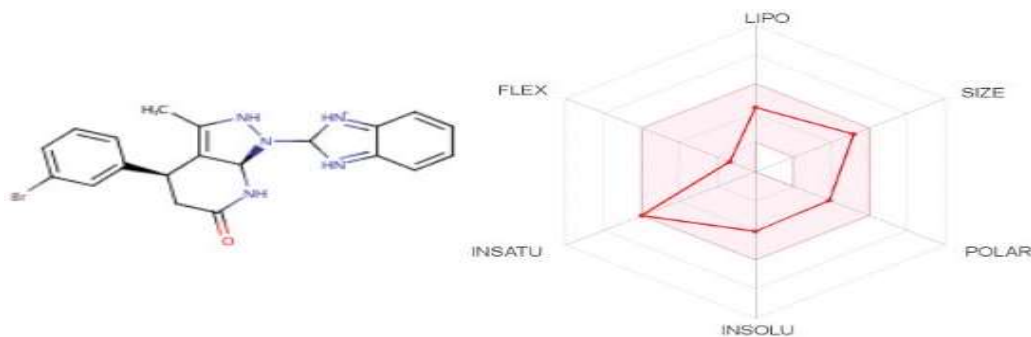
**Fig. 8. The bioavailability radar of ZINC64450313 using Swiss ADME predictor.**

The amount of gastrointestinal absorption of ZINC64450313 and its degree to permeate blood-brain barrier (BBB) was evaluated using the boiled egg model. As shown in Fig. 9, the yellow (yolk) region predicts ease of penetration of ZINC64450313 through the BBB, whilst the white zone suggests high passive gastrointestinal absorption.
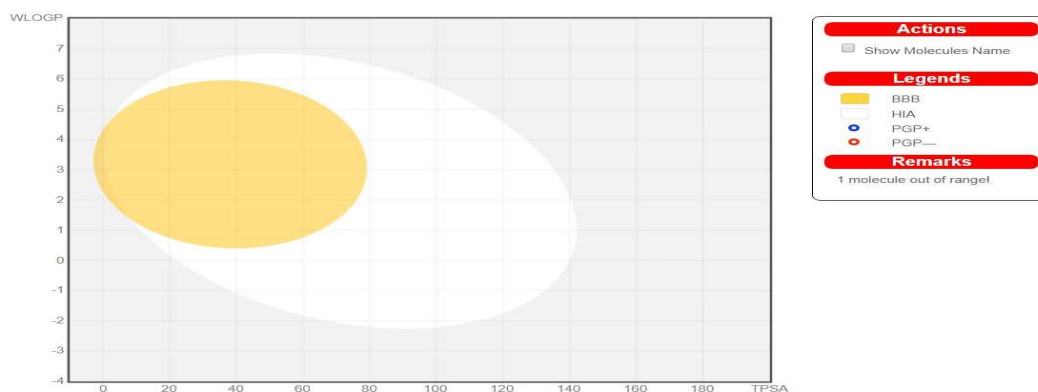
Fig. 9. Molecule falling in egg's yolk prediction of ZINC64450313.

A variety of scale was used to assess the solubility of ZINC64450313. As shown in Table 3, ZINC64450313 was observed to be moderately soluble. In a bid to exhaustively assess the pharmacokinetics of ZINC64450313, the lead molecule was observed to inhibit CYP3A4 (see Table 4). However, CYP 1A2, CYP2C9, CYP2D6 and CYP2C19 isoenzyme were not inhibited by ZINC64450313. Hence, drug-drug interactions that can lead to toxic ADME process *via* accumulation of metabolites is prevented. Furthermore, investigation of the druglikeness of the lead molecule (ZINC64450313) revealed that the Lipinski, Egan, Verber and Muegge rules were obeyed (see Table 5). On the contrary, Ghose rule was not obeyed as a violation was noticed.

Table 3: Water solubility of ZINC64450313.

Log S (ESOL)		-4.06
	Solubility	$3.72e^{-02}$ mg ml^{-1}; $8.72e^{-05}$ mol ml^{-1}
	Class	Moderately soluble
Log S (Ali)		-3.34
	Solubility	$1.94e^{-1}$ mg ml^{-1}; $4.55e^{-04}$ mol ml^{-1}
	Class	soluble
Log S (SILICOS-IT)		-6.69
	Solubility	$8.72e^{-02}$ mgml^{-1}; $2.05e^{-07}$ mol ml^{-1}
	Class	Poorly soluble

Table 4. Pharmacokinetics of ZINC64450313.

GI adsorption	Low
BBB permeant	No
P-gp substrate	Yes
CYP 1A2	No
CYP2C19	No
CYP2C9	No
CYP2D6	No
CYP3A4	Yes
Log Kp (skin permeation)	-7.35 cm s^{-1}

In the preclinical and clinical stages of drug development, toxicity assay of a drug is important. The ProTox-II online webserver was used to assess the toxicity risks associated with ZINC64450313. As shown in Fig. 10, ZINC64450313 was noticed to have an LD50 value of 10 mg/kg and belong to toxicity class 2. The assay was obtained with an average similarity index of 33.25% and prediction accuracy of 23%.

Table 5. Druglikeness of ZINC64450313.

Lipinski	Yes, 0 violation
Ghose	No: 1 violation: WLOGP<-0.4
Veber	Yes
Egan	Yes
Muegge	Yes
Bioavailability score	0.55
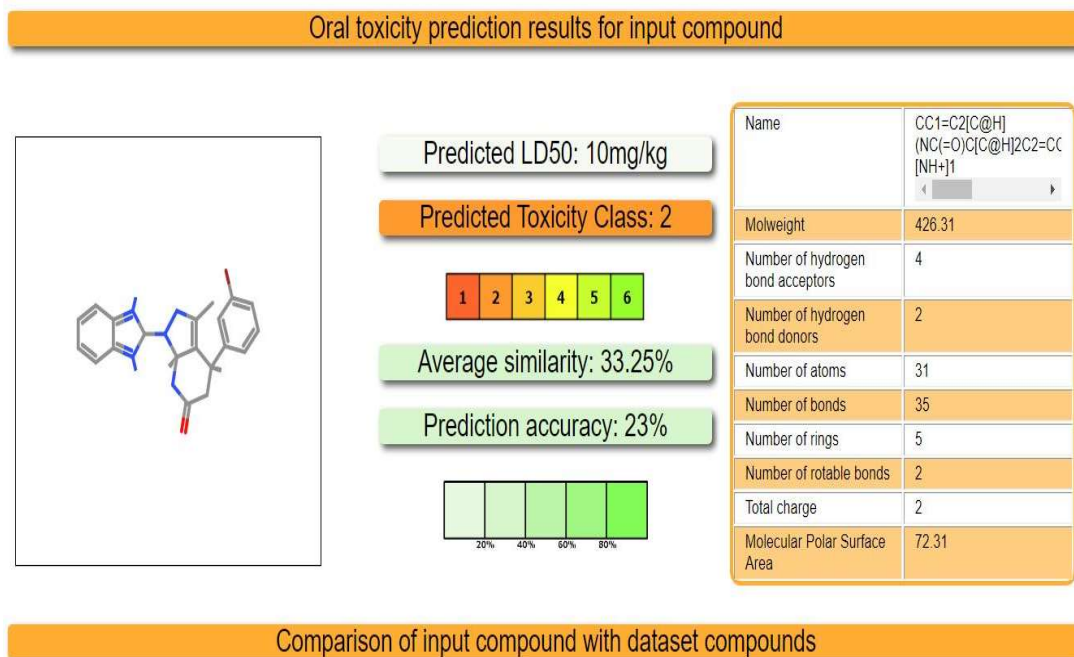
Fig. 10. The oral toxicity prediction of ZINC64450313.

3.4   *Frontier orbital analysis*

Frontier molecular orbital energies (HOMO and LUMO energies) were used to assess chemical reactivity descriptors of ZINC64450313 and ribavirin. The energy of the HOMO (E_{HOMO}) is associate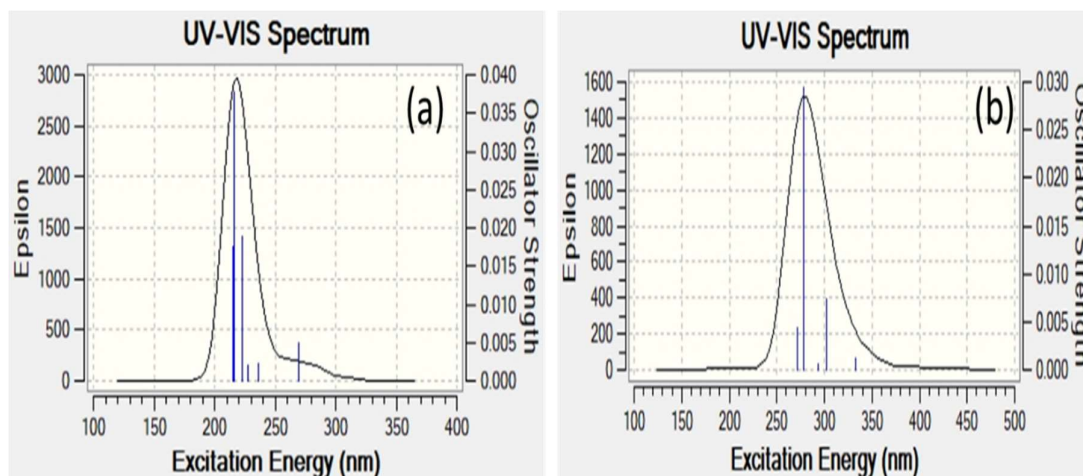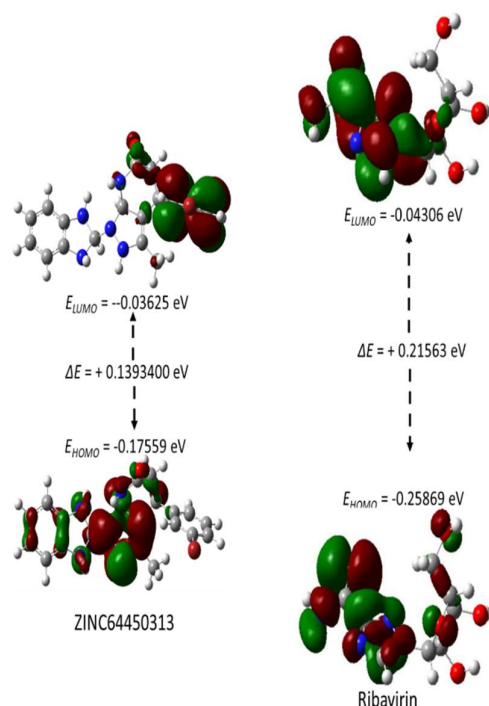d with ionization potential and energy of the LUMO (E_{LUMO}) is directly related to reactivity. The formation of transition state and chemical stability of some reaction processes is dependent on the interaction between these frontier orbitals.   The stability index was determined from the HOMO-LUMO energy gap ($\Delta E = E_{LUMO} - E_{HOMO}$), which is an important stability index (Srivastava *et al*., 2016). As shown in Table 6, the energy band gaps of ZINC64450313 and ribavirin were 0.13934 eV and 0.21563 eV respectively. A small energy band gaps indicate low stability (soft) and large gap suggest high stability (hard). A molecule with a small energy band gaps is easily polarizable (reactive) and is generally associated with high chemical reactivity.

Fig.11 The predicted UV-VIS spectra of (a) Ribavirin and (b) ZINC64450313

$E_{LUMO} = -0.04306$ eV

$E_{LUMO} = -0.03625$ eV

$\Delta E = +0.21563$ eV

$\Delta E = +0.1393400$ eV

$E_{HOMO} = -0.17559$ eV

$E_{HOMO} = -0.25869$ eV

ZINC64450313

Ribavirin

Fig.12: HOMO, LUMO orbitals at the B3LYP/6-311++G (d, p) basis set for ribavirin and ZINC64450313.

The stability of molecule can also be associated with hardness, the lower stability shows that the molecule is softer and hence more reactive. The global hardness of ribavirin is higher than that of lead molecule (ZINC64450313), indicating that the ZINC64450313 will be softer and more reactive than ribavirin (see Table 6).

Table 6: HOMO-LUMO energies and calculated global reactivity parameters of ZINC64450313and Ribavirin molecule, calculated by B3LYP/6-311++G (d,p) method

Parameters	ZINC64450313	Ribavirin
E_{HOMO} (eV)	-0.17559	-0.25869
E_{LUMO} (ev)	-0.03625	-0.04306
Energy gap (eV)	0.13934	0.21563
Electronegativity (χ)	0.10592	0.15088
Chemical hardness(η)	0.06967	0.10782
Softness(S)	14.3534	9.2750
Chemical potential	-0.06967	-0.10782
Electrophilicity index	0.03484	0.05391

This further explains why the ZINC64450313 interacted with more amino acids residues within

the pocket and had a higher docking score than ribavirin (see Table 2).

The predicted UV-VIS spectra of ribavirin and ZINC64450313 revealed close wavelength maxima of absorption (see Fig 11). This indicates the effectiveness of the virtual screening step, as both molecules are expected to have similar pharmacophoric features.

4.0 Conclusion

This paper demonstrates the application of computer-aided drug design techniques in the search for small molecules with inhibitory activities against Lassa fever nucleoprotien. Molecular docking results indicated that five compounds (ZINC64450313, ZINC00658482, ZINC40789449, ZINC14551223 and ZINC73892903) bind firmly to 3mx5 than ribavirin (reference molecule). Among all these predicted molecules and ribavirin, ZINC64450313 have demonstrated better reactivity index, moderate pharmacokinetic properties and druglikeness characteristics. Hence, there are indications that ZINC64450313 can inhibit the function of some essential protein(s) of 3mx5 that are essential to the viral life cycle. In other to meet the exigent demand for Lassa fever vaccine/drug, we recommend *in vitro* and *in vivo* assay of ZINC64450313.

5.0 References

Abdullahi, M., Olotu, F. A., & Soliman, M. E. (2018). Allosteric inhibition abrogates dysregulated LFA-1 activation: Structural insight into mechanisms of diminished immunologic disease. *Computational biology and chemistry, 73*, pp.49-56.

Ashburn, T. T., & Thor, K. B. (2004). Drug repositioning: identifying and developing new uses for existing drugs. *Nature reviews Drug discovery, 3,* 8, pp.673-683.

Ayers, P. W., & Levy, M. (2000). Perspective on "Density functional approach to the frontier-electron theory of chemical reactivity". *Theoretical Chemistry Accounts,* 103, 3-4, pp. 353-360.

Baize, S., Kaplon, J., Faure, C., Pannetier, D., Georges-Courbot, M.-C., & Deubel, V. (2004). Lassa virus infection of human dendritic cells and macrophages is productive but fails to activate cells. *The Journal of Immunology,* 172, 5, pp. 2861-2869.

Becke, A. D. (2005). Real-space post-Hartree–Fock correlation models. *The Journal of Chemical Physics,* 122, 1-6, pp. 064101.

Bederka, L. H., Bonhomme, C. J., Ling, E. L., & Buchmeier, M. J. (2014). Arenavirus stable signal peptide is the keystone subunit for glycoprotein complex organization. *MBio,* 5, 6, pp. e02063-02014.

Carrillo-Bustamante, P., Nguyen, T. H. T., Oestereich, L., Günther, S., Guedj, J., & *Graw*, F. (2017). Determining Ribavirin's mechanism of action against Lassa virus infection. *Scientific reports,* 7, 1, pp. 1-12.

Chattaraj, P. K., Chakraborty, A., & Giri, S. (2009). Net electrophilicity. *The Journal of Physical Chemistry A,* 113, 37, pp. 10068-10074.

Cheng, F., Murray, J. L., & Rubin, D. H. (2016). Drug repurposing: new treatments for zika virus infection? *Trends in molecular medicine,* 22, 11, pp. 919-921.

Chermette, H. (1999). Chemical reactivity indexes in density functional theory. *Journal of computational chemistry,* 20, 1, pp. 129-154.

Dyall, J., Coleman, C. M., Hart, B. J., Venkataraman, T., Holbrook, M. R., Kindrachuk, J., Laidlaw, M. (2014). Repurposing of clinically developed drugs for treatment of Middle East respiratory syndrome coronavirus infection. *Antimicrobial agents and chemotherapy,* 58, 8, pp. 4885-4893.

Gaussian09, R. A. (2009). M.J. Frisch, G.W. Trucks, H.B. Schlegel, G.E. Scuseria, M.A. Robb, J.R. Cheeseman, J.A. Gonzalez, J.A. Pople, Gaussian 09, Revision E.01, Gaussian, Inc, Wallingford, CT, 2004. *Inc., Wallingford CT,* 121, pp. 150-166.

Gazquez, J. L., Cedillo, A., & Vela, A. (2007). Electrodonating and electroaccepting powers. *The Journal of Physical Chemistry A,* 111, 10, pp. 1966-1970.

Geerlings, P., De Proft, F., & Langenaeker, W. (2003). Conceptual density functional theory. *Chemical Reviews,* 103, 5, pp. 1793-1874.

Hanwell, M. D., Curtis, D. E., Lonie, D. C., Vandermeersch, T., Zurek, E., & Hutchison, G. R. (2012). Avogadro: an advanced semantic chemical editor, visualization, and analysis platform. *Journal of cheminformatics,* 4, 1, pp.1-17.

Hastie, K. M., Zandonatti, M. A., Kleinfelter, L. M., Heinrich, M. L., Rowland, M. M., Chandran, K., Saphire, E. O. (2017). Structural basis for antibody-mediated neutralization of Lassa virus. *Science,* 356, 6341, pp. 923-928.

Houlihan, C., & Behrens, R. (2017). Lassa fever. *Bmj,* 358, 1-6, pp. j2986.

Johansen, L. M., DeWald, L. E., Shoemaker, C. J., Hoffstrom, B. G., Lear-Rooney, C. M., Stossel, A., Grenier, J. M. (2015). A screen of approved drugs and molecular probes identifies therapeutics with anti–Ebola virus activity. *Science translational medicine,* 7, 290, pp. 290ra289-290ra289.

Keenlyside, R. A., McCormick, J. B., Webb, P. A., Smith, E., Elliott, L., & Johnson, K. M. (1983). Case-control study of Mastomys natalensis and humans in Lassa virus-infected households in Sierra Leone. *The American Journal of Tropical Medicine and Hygiene,* 32, 4, 829-837.

Koes, D. R., & Camacho, C. J. (2012). *ZINCPharmer: pharmacophore search of the ZINC database. Nucleic acids research, 40*(W1), W409-W414.

Koopmans, T. (1934). Über die Zuordnung von Wellenfunktionen und Eigenwerten zu den einzelnen Elektronen eines Atoms. *Physica,* 1, 1-6, pp. 104-113.

Kouznetsova, J., Sun, W., Martínez-Romero, C., Tawa, G., Shinn, P., Chen, C. Z., Zheng, W. (2014). Identification of 53 compounds that block Ebola virus-like particle entry via a repurposing screen of approved drugs. *Emerging microbes & infections,* 3, 1, pp. 1-7.

Lukashevich, I. S., Maryankova, R., Vladyko, A. S., Nashkevich, N., Koleda, S., Djavani, M.,. Salvato, M. S. (1999). Lassa and mopeia virus replication in human monocytes/macrophages and in endothelial cells: Different effects on IL-8 and TNF-α gene expression. *Journal of mMedical Virology,* 59, 4, pp. 552-560.

Madrid, P. B., Chopra, S., Manger, I. D., Gilfillan, L., Keepers, T. R., Shurtleff, A. C., Davey, R. A. (2013). A systematic screen of FDA-approved drugs for inhibitors of biological threat agents. *PLoS ONE, 8, 4, pp.*1-9 .

Mahanty, S., Hutchinson, K., Agarwal, S., Mcrae, M., Rollin, P. E., & Pulendran, B. (2003). Cutting edge: impairment of dendritic cells and *adaptive* immunity by Ebola and Lassa viruses. *The Journal of Immunology,* 170, 6, pp. 2797-2801.

McCormick, J., King, I., Webb, P., Scribner, C., Craven, R., Johnson, K., Belmont-Williams, R. (1986). Effective therapy with ribavirin. *New England Journal of Medicine,* 314, pp. 20-26.

McCormick, J. B., Walker, D. H., King, I. J., Webb, P. A., Elliott, L. H., Whitfield, S. G., & Johnson, K. M. (1986). Lassa virus hepatitis: a study of fatal Lassa fever in humans. *The American journal of tropical medicine and hygiene,* 35, 2, pp. 401-407.

Monath, T. P., Newhouse, V. F., Kemp, G. E., Setzer, H. W., & Cacciapuoti, A. (1974). Lassa virus isolation from Mastomys natalensis rodents during an epidemic in Sierra Leone. *Science,* 185, 4147, pp. 263-265.

Monteiro, A., Scotti, M., & Scotti, L. (2019). *Molecular docking of fructose-derived nucleoside analogs against reverse transcriptase of HIV-1.* Paper presented at the Proceedings of MOL2NET 2019, International Conference on Multidisciplinary Sciences, 5th edition.

Morris, G. M., Goodsell, D. S., Halliday, R. S., Huey, R., Hart, W. E., Belew, R. K., & Olson, A. J. (1998). Automated docking using a Lamarckian genetic algorithm and an empirical binding free energy function. *Journal of computational chemistry,* 19, 14, pp. 1639-1662.

Pandey, M., Muthu, S., & Gowda, N. N. (2017). Quantum mechanical and spectroscopic (FT-IR, FT-Raman, 1H, 13C NMR, UV-Vis) studies, NBO, NLO, HOMO, LUMO and Fukui function analysis of 5-Methoxy-1H-benzo [d] imidazole-2 (3H)-thione by DFT studies. *Journal of Molecular Structure,* 1130, pp. 511-521.

Patil, R., Das, S., Stanley, A., Yadav, L., Sudhakar, A., & Varma, A. K. (2010). Optimized hydrophobic interactions and hydrogen bonding at the target-ligand interface leads the pathways of drug-designing. *PLoS ONE,* 5, 8, pp. 1-8

Pettersen, E. F., Goddard, T. D., Huang, C. C., Couch, G. S., Greenblatt, D. M., Meng, E. C., & Ferrin, T. E. (2004). UCSF Chimera—a visualization system for exploratory research and analysis. *Journal of computational chemistry, 25*(13), 1605-1612.

Sahoo, M., Lingaraja Jena, S. D., & Kumar, S. (2016). Virtual screening for potential inhibitors of NS3 protein of Zika virus. *Genomics & informatics, 14*(3), 104.

Sbrana, E., Mateo, R. I., Xiao, S.-Y., Popov, V. L., Newman, P. C., & Tesh, R. B. (2006). Clinical laboratory, virologic, and pathologic changes in hamsters experimentally infected with Pirital virus (Arenaviridae): a rodent model of Lassa fever. *The American journal of tropical medicine and hygiene,* 74, 6, pp. 1096-1102.

Shimojima, M., Ströher, U., Ebihara, H., Feldmann, H., & Kawaoka, Y. (2012). Identification of cell surface molecules involved in dystroglycan-independent Lassa virus cell entry. *Journal of virology,* 86, 4, pp. 2067-2078.

Srivastava, K., Shimpi, M. R., Srivastava, A., Tandon, P., Sinha, K., & Velaga, S. P. (2016). Vibrational analysis and chemical activity of paracetamol–oxalic acid cocrystal based on monomer and dimer calculations: DFT and AIM approach. *RSC Advances,* 6, 12, pp. 10024-10037.

Walker, D., McCormick, J., Johnson, K., Webb, P., Komba-Kono, G., Elliott, L., & Gardner, J. (1982). Pathologic and virologic study of fatal Lassa fever in man. *The American journal of pathology*, 107,3, pp.349.

Yang, W., & Parr, R. G. (1985). Hardness, softness, and the fukui function in the electronic theory of metals and catalysis. *Proceedings of the National Academy of Sciences,* 82, 20, pp. 6723-6726.

Zhang, X., Yan, F., Tang, K., Chen, Q., Guo, J., Zhu, W., Guo, Y. (2019). Identification of a clinical compound losmapimod that blocks Lassa virus entry. *Antiviral research,* 167, pp. 68-77.